Measurement of upconversion in Er:YAG via *z*-scan

Jeffrey O. White[1,*] and Carl E. Mungan[2]

[1]*Army Research Laboratory, 2800 Powder Mill Road, Adelphi, Maryland 20783-1197*
[2]*Physics Department, United States Naval Academy, Annapolis, Maryland 21402-1363*
**Corresponding author: jeffrey.owen.white@us.army.mil*

Received July 8, 2011; accepted August 2, 2011;
posted August 9, 2011 (Doc. ID 150790); published September 5, 2011

We demonstrate the use of the *z*-scan technique for measuring the upconversion coefficient in Er:YAG. The upconversion coefficient is found to be linearly proportional to the concentration for samples of concentration 0.5–3.0 at.%. A fit to four samples at room temperature yields a value of $C_{\mathrm{up}} = (2.0 \pm 0.5) \times 10^{-17}\,\mathrm{cm}^3/\mathrm{s/at.\%}$. The coefficient at liquid-nitrogen temperatures is $C_{\mathrm{up}} = (9.5 \pm 2.4) \times 10^{-17}\,\mathrm{cm}^3/\mathrm{s/at.\%}$. © 2011 Optical Society of America

OCIS codes: 190.7220, 140.3500, 300.6460.

1. INTRODUCTION

Cooperative, or energy-transfer, upconversion reduces the population of the $^4\mathrm{I}_{13/2}$ manifold in Er:YAG, increasing the laser threshold but not, in theory, the slope efficiency [1]. In the present paper, the cooperative upconversion parameter in Er:YAG is measured using the *z*-scan technique as a function of Er concentration (0.5–3 at.%) with the sample at room temperature (298 K) and at 80 K. The value at 80 K is approximately five times larger than the value at room temperature.

Er:YAG lasers are of interest because they can emit at the eye-safe wavelength of 1645 nm. When pumped at 1532 nm, they have a quantum defect of only 7%. Er:YAG, at this choice of pump and laser wavelengths, is thermodynamically a 2.4-level laser at room temperature, and a 2.6-level laser at 77 K [2]. An Er:YAG laser operating at cryogenic temperatures has recently produced 400 W at 1645 nm [3]. Knowledge of the low-temperature upconversion coefficient will allow further improvements in the design. It may also help explain the unusual temperature-dependent output power, which peaks at ~160 K [4].

C_{up} was estimated to be $1\text{–}3 \times 10^{-16}\,\mathrm{cm}^3/\mathrm{s}$ for a 1% sample of Er:YAG, based on early measurements of the fluorescence decay rate and the increase in laser threshold [5,6]. A value of $C_{\mathrm{up}} = 5 \times 10^{-18}\,\mathrm{cm}^3/\mathrm{s/at.\%}$ was previously obtained with a time-dependent method based on the nonexponential decay of the fluorescence from the $^4\mathrm{I}_{13/2}$ level [7]. A value of $3.5 \times 10^{-18}\,\mathrm{cm}^3/\mathrm{s/at.\%}$ was found using a steady-state method based on the upconversion-induced increase in the lasing threshold [8]. Relative to the time-resolved technique for measuring C_{up}, the advantage of the *z*-scan method is that it can be performed with a cw or quasi-cw source. Relative to the laser threshold technique, the advantage of the *z*-scan method is that it does not require a long laser-quality rod, output couplers, or careful alignment of a cavity. A key merit of the *z*-scan technique is that the source can be the same diode used to pump an Er:YAG laser. However, a diffraction-limited beam, and high optical quality, homogeneous samples of ~10 mm diameter are required.

2. MODEL

A model including the lowest four manifolds of Er^{3+} ($^4\mathrm{I}_{15/2}$, $^4\mathrm{I}_{13/2}$, $^4\mathrm{I}_{11/2}$, and $^4\mathrm{I}_{9/2}$) is used to fit the data (Fig. 1). Included in the model is a rate equation for the population of each manifold, N_i, where i runs from 1 to 4. The laser absorption and stimulated emission are between the lowest two manifolds. The rate equations for the four manifolds are

$$\frac{dN_1}{dt} = +\frac{I\sigma}{h\nu}(f_{\mathrm{e}}N_2 - f_{\mathrm{a}}N_1) + N_2W_{21} + N_3W_{31} + N_4W_{41} + C_{\mathrm{up}}N_2^2, \tag{1}$$

$$\frac{dN_2}{dt} = -\frac{I\sigma}{h\nu}(f_{\mathrm{e}}N_2 - f_{\mathrm{a}}N_1) - N_2W_{21} + N_3W_{32} + N_4W_{42} - 2C_{\mathrm{up}}N_2^2, \tag{2}$$

$$\frac{dN_3}{dt} = N_4W_{43} - N_3(W_{32} + W_{31}), \tag{3}$$

$$\frac{dN_4}{dt} = C_{\mathrm{up}}N_2^2 - N_4(W_{43} + W_{42} + W_{41}). \tag{4}$$

Here, I is the laser intensity, σ is the absolute cross section, W_{ij} is the relaxation rate from level i to level j, C_{up} is the upconversion coefficient, and $f_a(f_e)$ is the probability given by the Boltzmann distribution that an ion in the $^4\mathrm{I}_{15/2}$ ($^4\mathrm{I}_{13/2}$) manifold is in the sublevel that can absorb (emit) a laser photon.

For Er:YAG at room temperature, the W_{32} and W_{43} rates are dominated by nonradiative relaxation; the other rates are dominated by radiative relaxation (Table 1). The W_{43} rate is estimated to be an order of magnitude larger than the W_{32} rate, but as long as W_{32} and W_{43} remain much larger than the other decay rates, their impact in a steady state is negligible. At 77 K, $W_{21} = 101\,\mathrm{Hz}$ [4]; we use the room-temperature values for the other radiative rates, assuming that the nonradiative rates remain large in comparison.

The values of $N_1(z)$ to $N_4(z)$ are obtained by solving Eqs. (1)–(4) in a steady state, simultaneously with a propagation equation for the laser beam

 © 2011 Optical Society of America

Table 1. Room-Temperature Relaxation Rates (Hz) Used in the Model

W_{21}	W_{31}	W_{32}	W_{41}	W_{42}	W_{43}
136 [4]	118 [11]	9000 [7]	51 [12]	57 [12]	10^5

$$\frac{dI}{dz} = I\sigma(f_e N_2 - f_a N_1) = -\alpha I. \tag{5}$$

To account for the Gaussian intensity profile, the pump beam is treated as a superposition of eight equally spaced intensities. The difference between eight slices and 16 was found to be negligible, so the smaller number was used to speed the calculations.

One assumption in the model is that the beam radius is constant across the 1 mm thickness of the sample. This simplifies the transmission calculations, and is supported by all samples having a thickness less than the confocal parameter or Rayleigh range. Scattering losses in the sample can be neglected because of their excellent optical quality. The model is local in the sense that the populations at any point in space are determined by the intensity at that point only, which assumes that the excitation energy migrates only a short distance compared to the beam diameter.

3. EXPERIMENT

The sample is illuminated at 1532.5 nm, which couples the second sublevel of the ground manifold to the lowest sublevel of the $^4I_{13/2}$ manifold. The source is a distributed feedback laser operating continuously and amplified in a single-mode fiber to 3 W. The duty cycle was reduced to 10% with a shutter operating at 1 Hz, to avoid heating the samples. An InGaAs photodiode and lock-in amplifier were used to detect the beam transmitted through the sample. The samples were 10 mm in diameter, 1 mm thick, and antireflection coated. The samples were placed in a cryostat for the 80 K measurements.

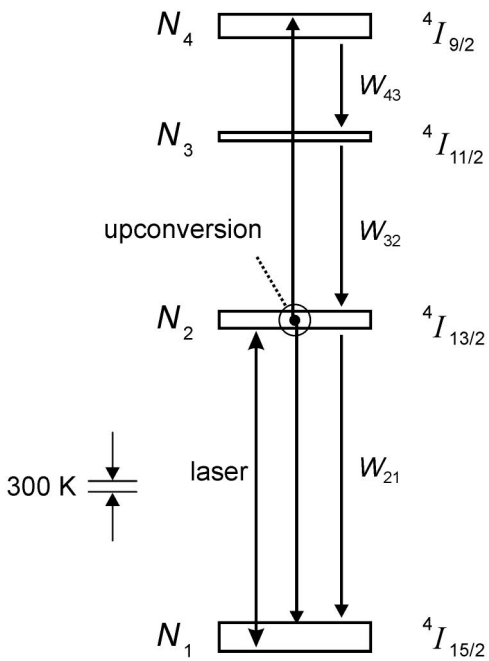

Fig. 1. Diagram of the four manifolds, the laser transition, the upconversion, and select relaxations.

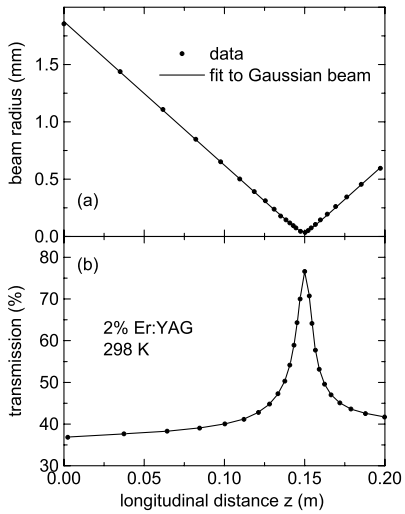

Fig. 2. (a) Beam radius as a function of position. (b) Transmission of a 2% Er:YAG sample at 298 K.

A standard z-scan geometry was used [9], with a 20 cm focal length doublet lens. The intensity profile was measured by translating a razor blade across the beam and fitting to an error function to determine the waist [Fig. 2(a)].

4. RESULTS

The transmission of each sample as a function of the position shows a peak where the beam intensity is highest, due to saturation of the absorption [Fig. 2(b)]. Upconversion depletes the $^4I_{13/2}$ manifold, lowering the peak, shifting the onset of saturation to higher intensities.

The shift in the saturation is evident in a plot of the effective absorption coefficient versus the peak intensity (Fig. 3) for a 1% sample (1.4×10^{20} ions/cm^3). Here, α_{eff} is calculated from the experimental data (symbols) according to

$$P(L) = P(0)\exp(-\alpha_{\mathrm{eff}} L), \tag{6}$$

where P is the laser power. The different symbols correspond to runs at different power levels. Simulation curves for $C_{\mathrm{up}} = 0$ (dashed line) and for $C_{\mathrm{up}} = 2 \times 10^{-17}$ cm^3/s (solid line) are also shown.

For a 1% sample at 80 K, the effective absorption coefficient versus the peak intensity is shown in Fig. 4, along with

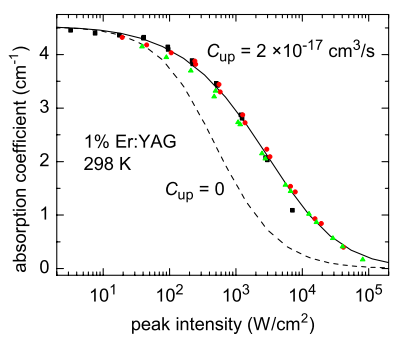

Fig. 3. (Color online) Effective absorption coefficient versus peak intensity for 1% Er:YAG at 298 K. The curves are simulations.

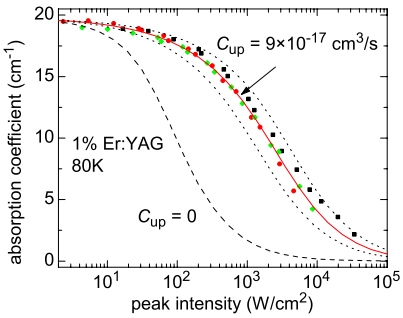

Fig. 4. (Color online) Erbium-doped YAG z-scan experimental data at 80 K at three different powers (symbols). The dotted lines represent values of C_{up} that differ from the solid line by a factor of 2.

simulation curves for $C_{up} = 0$ (dashed line) and for $C_{up} = 9 \times 10^{-17}\,\mathrm{cm}^3/\mathrm{s}$ (solid line). These are the first published measurements of Er:YAG upconversion at cryogenic temperatures.

The results for a variety of samples indicate that C_{up} is approximately proportional to the Er concentration at both temperatures (Fig. 5). A linear fit to the four samples at room temperature yields a value of $C_{up} = (2.0 \pm 0.5) \times 10^{-17}\,\mathrm{cm}^3/\mathrm{s/at.\%}$. The corresponding value at 80 K is $C_{up} = (9.5 \pm 2.4) \times 10^{-17}\,\mathrm{cm}^3/\mathrm{s/at.\%}$

5. DISCUSSION

Two constraints on using the z-scan technique to measure upconversion are the slow sample response time and sample heating. The pump duration needs to be long compared to the time to reach a steady state, but short compared to the time during which sample heating would affect the transmission. In the part of the scan where the intensity is low, the time to reach a steady state is long, but the change in transmission due to saturation is small, so the constraints are relatively easy to accommodate. In the part of the scan where the intensity is high, the saturation is significant, but the time to reach a steady state is short, so the constraints are, again, easy to accommodate. In the range of the scan where the intensity is intermediate in value, the constraints become important. In the present experiments, an exposure time of 0.1 s was found to be long enough to reach a steady state, but short enough to avoid sample heating, provided the duty cycle was below 10% and $\alpha_0 L$ was less than ~2. At 80 K, the source was tuned off resonance, as otherwise the large peak value in the (absolute) absorption cross section of $\sigma = 2.48 \times 10^{-18}\mathrm{cm}^2$ [10] caused noticeable sample heating during the experimental runs.

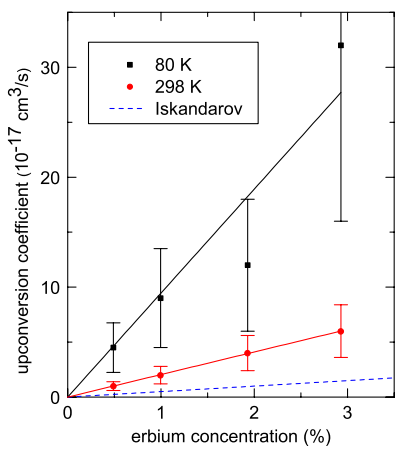

Fig. 5. (Color online) Measured upconversion coefficient (symbols) as a function of Er concentration at 80 and 298 K, along with linear fits to each. The dashed line is a linear fit to the low-concentration results of [7].

6. CONCLUSIONS

z-scan measurements of Er:YAG have been made at room temperature and at 80 K. The data have been interpreted with a steady-state model, including rate equations for the (intensity-dependent) populations of the lowest four manifolds, and an equation for the (population-dependent) propagation of the light. The resulting room temperature value of $C_{up} = (2.0 \pm 0.5) \times 10^{-17}\,\mathrm{cm}^3/\mathrm{s/at.\%}$ doping is approximately four times the value obtained in [7]. Data taken at 80 K yield $C_{up} = (9.5 \pm 2.4) \times 10^{-17}\,\mathrm{cm}^3/\mathrm{s/at.\%}$, and are the first published measurements at cryogenic temperatures.

High-power erbium-doped lasers for eye-safe applications are currently being designed to operate at cryogenic temperatures because the optical, thermal, and mechanical properties of Er:YAG, for example, improve as the temperature is lowered, depending on the particular transitions involved. Knowledge of the low-temperature value of C_{up} and of its dependence on the Er concentration will allow the effect of upconversion to be minimized by choosing an optimal level of doping. An advantage of the z-scan technique for measuring upconversion is that it can be carried out with the same quasi-cw diode laser that is commonly used to pump an Er:YAG laser.

ACKNOWLEDGMENTS

We are grateful for the assistance of Robert Dibiano, Alexander B. Fick, Thomas A. Mercier, Jr., and John E. McElhenny with data acquisition and programming.

REFERENCES AND NOTES

1. J. O. White, M. Dubinskii, L. D. Merkle, I. Kudryashov, and D. Garbuzov, "Resonant pumping and upconversion in 1.6 μm Er^{3+} lasers," J. Opt. Soc. Am. B **24**, 2454–2460 (2007).
2. J. O. White, "Parameters for quantitative comparison of two-, three-, and four-level laser media, operating wavelengths, and temperatures," IEEE J. Quantum Electron. **45**, 1213–1220 (2009).
3. S. Setzler, M. J. Shaw, M. J. Kukla, J. R. Unternahrer, K. M. Dinndorf, J. A. Beattie, and E. P. Chicklis, "A 400 W cryogenic Er:YAG slab laser at 1645 nm," Proc. SPIE **7686**, 76860C (2010).
4. N. Ter-Gabrielyan, M. Dubinskii, G. A. Newburgh, A. Michael, and L. D. Merkle, "Temperature dependence of a diode-pumped cryogenic Er:YAG laser," Opt. Express **17**, 7159–7169 (2009).
5. D. K. Killinger, "Effect of phonon-assisted upconversion on 1.64 μm Er:YAG laser performance," Quarterly Progress Rep. (Lincoln Laboratory Solid-State, 1987), Section 2.2, pp. 13–16.
6. D. K. Killinger, "Phonon-assisted upconversion in 1.64 μm Er:YAG lasers," in *Conference on Lasers and Electro-Optics* of 1987 OSA Technical Digest Series (Optical Society of America, 1987), paper THJ4.
7. M. O. Iskandarov, A. A. Nikitichev, and A. I. Stepanov, "Quasi-two-level Er^{3+}:$Y_3Al_5O_{12}$ laser for the 1.6 μm range," J. Opt. Technol. **68**, 885–888 (2001).
8. J. W. Kim, J. I. Mackenzie, and W. A. Clarkson, "Influence of energy-transfer-upconversion on threshold pump power in quasi-three-level solid state lasers," Opt. Express **17**, 11935–11943 (2009).
9. M. Sheik-Bahae, A. A. Said, T. H. Wei, D. J. Hagan, and E. W. Van Stryland, "Sensitive measurements of optical nonlinearities

using a single beam," IEEE J. Quantum Electron. **26**, 760–769 (1990).

10. This value was calculated as $\sigma = \alpha_0/Nf_a$, where $f_a = 0.300$, for a sample of concentration $N = 6.80 \times 10^{19}\,\mathrm{cm}^{-3}$. The unsaturated absorption coefficient was measured at 80 K to be $\alpha_0 = 50.6\,\mathrm{cm}^{-1}$.
11. D. K. Sardar, C. C. Russell III, J. B. Gruber, and T. H. Allik, "Absorption intensities and emission cross sections of principal intermanifold and inter-Stark transitions of $Er^{3+}(4f^{11})$ in polycrystalline ceramic garnet $Y_3Al_5O_{12}$," J. Appl. Phys. **97**, 123501 (2005).
12. D. K. Sardar, W. M. Bradley, J. J. Perez, J. B. Gruber, B. Zandi, J. A. Hutchinson, C. W. Trussell, and M. R. Kokta, "Judd-Ofelt analysis of the $Er^{3+}(4f^{11})$) absorption intensities in Er^{3+}-doped garnets," J. Appl. Phys. **93**, 2602–2607 (2003).